View metadata, citation and similar papers at core.ac.uk
brought to you by CORE
provided by University of Missouri: MOspace

Peroxiredoxin 2 and peroxidase enzymatic activity of mammalian spermatozoa

Gaurishankar Manandhar[1], Antonio Miranda-Vizuete[2], Jose R Pedrajas[3], William J Krause[4], Shawn Zimmerman[1], Miriam Sutovsky[1], Peter Sutovsky[1,5]

[1]Division of Animal Sciences, [4]Dept. of Pathology & Anatomical Sciences, and [5]Dept. of ObstetricsGynecology and woman's health, University of Missouri-Columbia, MO, USA; [2] Centro Andaluz de Biología del Desarrollo (CABD-CSIC) Departamento de Fisiologia, Anatomia y Biologia Celular, Universidad Pablo de Olavide , 41013 Sevilla, Spain, [3]Departamento de Biología Experimental, Facultad de Ciencias Experimentales, Universidad de Jaén, Jaén, Spain

Running title: Mammalian sperm peroxiredoxin 2

Key words: Spermatozoa, Peroxiredoxin 2, Reactive oxygen, Sperm proteome, Diethyl maleate, Carmustin

Correspondence: G Manandhar, University of Missouri, Division of Animal Sciences, S141 ASRC, Columbia, MO 65211 Email: manandharg@missouri.edu

Abstract

Peroxiredoxin 2 (PRDX2) is a highly efficient redox protein that neutralizes hydrogen peroxide resulting in protection of cells from oxidative damage and regulation of peroxide-mediated signal transduction events. The oxidized form of PRDX2 is reverted back to the reduced form by the thioredoxin system. In the present study, we investigated the presence of PRDX2 in mouse and boar spermatozoa as well as in mouse spermatids using proteomic techniques and immunocytochemistry. Sperm and spermatid extracts displayed 20 kDa PRDX2 band in Western blotting. PRDX2 occurred as a Triton soluble form in the spermatids and as an insoluble form in mature spermatozoa. Boar seminiferous tubule extracts were immunoprecipitated with PRDX2 antibody and separated by SDS PAGE. Peptide mass fingerprinting by MALDI-TOF and microsequencing by nanospray QqTOF MS/MS revealed the presence of PRDX2 ions in the immunoprecipitated band along with sperm mitochondria associated cysteine rich protein, cellular nucleic acid binding protein and glutathione peroxidase 4. In mouse spermatocytes and spermatids, diffuse labeling of PRDX2 was observed in the cytoplasm and residual bodies. After spermiation PRDX2 localization became confined to the mitochondrial sheath of the sperm tail midpiece. Boar spermatozoa displayed similar PRDX2 localization as in mouse spermatozoa. Boar spermatozoa with disrupted acrosomes expressed PRDX2 in the postacrosomal sheath region. Peroxidase enzyme activity of boar sperm extracts was evaluated by estimating the rate of NADPH oxidation in the presence or absence of a glutathione depletor (diethyl maleate) or a glutathione reductase inhibitor (carmustin). Diethyl maleate partially inhibited peroxidase activity while carmustin showed an insignificant effect. These observations suggest that glutathione and glutathione reductase activity contribute only partially to the total peroxidase activity of the sperm extract. While the specific role of PRDX2 in the total peroxidase activity of sperm extract is still an open question, the present study for the first time shows the presence of PRDX2 in mammalian spermatozoa. Peroxidase activity in sperm extracts is not due to the glutathione system and therefore possibly contributed by PRDX2 and other peroxiredoxins.

Copyright 2009 by The Society for the Study of Reproduction.

Introduction

Oxidative stress is one of the major constrains mammalian spermatozoa encounter during development in the testis, maturation in the epididymis and capacitation in the female reproductive tract. Reactive oxygen species (ROS) in male and female reproductive tracts cause a wide spectrum of damages to spermatozoa. At high concentrations, ROS cause peroxidation of unsaturated fatty acids of the plasma membrane leading to structural breakdown or functional pathology. ROS also cause single or double stranded DNA breaks resulting in apoptosis [1]. In general, elevated ROS is associated with a decline of semen quality or infertility [2] while low concentration of ROS plays a useful role in regulating several transmembrane signal transduction pathways in somatic cells [3], acrosome reaction and capacitation in spermatozoa [4, 5]. Tight packaging of sperm chromatin is ensured by oxidation and cross-linking of thiol groups of sperm nuclear protamines, a process probably regulated by nuclear-localized glutathione peroxidase-4 through fine tuning of ROS concentrations [6].

Larger surges of ROS in the male or female reproductive tracts are usually controlled by the enzymes superoxide dismutase (SOD) and catalase [7, 8]. SOD converts superoxide anion into H_2O_2 which is membrane permeant, and carried to the peroxisomes where it is neutralized by catalase. Non-protein thiols particularly glutahione (GSH) neutralize various kinds of ROS or reduce proteins denatured by ROS into their native form. Reproductive cells are also equipped with a series of redox proteins and enzymes that specialize in neutralizing minor surges of ROS and modulating general ROS concentrations. Thioredoxins (TRX) and peroxiredoxins (PRDX) are the prevalent redox proteins occurring in a wide variety of tissues and cells [9, 10]. Sperm specific thioredoxins (SPTRX, official symbol TXNDC) have been identified in human and mouse spermatozoa as well as in the developing testicular germ cells [11, 12].

The PRDX proteins belong to a unique class of redox proteins that react with hydrogen peroxide via the sulfhydryl radical (–SH) of their conserved peroxidatic cysteine residue (C_p). As a result, the C_p is oxidized to cysteine sulfenic acid (C_p-SOH) which then interacts with the resolving cysteine (C_r) of another PRDX forming interdisulphide bonds between two molecules (C_p-S—S-C_r) resulting in a homodimer [13]. In mammals, six isoforms of PRDX (named as PRDX1 through PRDX6) have been identified [14]. The isoforms PRDX1-PRDX5 are called 2-cys PRDX due to the presence of two conserved cysteine groups. PRDX6 has only one conserved cysteine, similar to the bacterial peroxiredoxins. PRDX2 (EC 1.11.1.15) is the third most abundant protein in mammalian erythrocytes [15] and accounts for a substantial portion of the total soluble protein in somatic cells [16]. PRDX2 is the fastest regenerating redox protein [17] and is more efficient in neutralizing H_2O_2 than catalase and glutathione peroxidase [18] as well as being more effective in protecting cells from H_2O_2 damage than glutathione peroxidase [19].

Transcripts of all PRDX have been found in mammalian reproductive organs [14]. The PRDX1 and PRDX2 transcripts and proteins occur in the Leydig and Sertoli cells of mouse testis, but spermatogonia and spermatocytes apparently do not express them [20]. It is not known whether these redox proteins are expressed by spermatids or whether mature spermatozoa retain them. Among six isoforms of PRDX, only PRDX4 and PRDX5 have been found in mammalian male gametes. The membrane bound form of PRDX4 is associated with the acrosomal vesicles of spermatids, and is possibly involved in acrosome biogenesis [21]. During spermatid elongation PRDX4 is discarded with the residual bodies and not detected in the mature spermatozoa. PRDX5 has been found in boar sperm acrosomal membrane fragments that interacted with the isolated porcine zona pellucida [22]. In the present work, we have investigated the presence of PRDX2 in spermatozoa and spermatids of mice and boar, its subcellular localization, and the peroxidase enzymatic activity of the sperm extracts.

Materials and Methods

Antibodies

Anti peroxiredoxin 2 mouse monoclonal antibody (mAb 1E8) was purchased from Abcam (www.abcam.com). It was produced against recombinant human protein purified from *E. coli.* A full length N-terminal His tagged recombinant human PRDX2 protein was procured from US Biological (www.usbio.net). Anti β-tubulin antibody E7 was purchased from Developmental Studies Hybridoma Bank (dshb.biology.uiowa.edu). Secondary antibodies conjugated to FITC, TRITC and HRP were procured from commercial sources (Zymed Lab Inc. www.invitrogen.com). Other reagents were purchased from Sigma (www.sigmaaldrich.com), unless otherwise mentioned. Chemical handling and disposal were done by following approved protocol from the Institutional Environmental Health & Safety Committee of the University of Missouri.

Animal handling and sample collection

Animals were handled by following an approved University of Missouri Animal Care and Use (ACUC) protocol. ICR mice were bred in house at the University of Missouri-Columbia by keeping in an environmentally controlled room with a 14-h light, 10-h dark cycle. Seven-to-ten weeks old male mice were euthanized by cervical dislocation for sperm and testis collection. Large White boars were bred and raised at the South Farm, University of Missouri – Columbia. Sperm ejaculates were collected from 9 months to 2 years old boars by a gloved hand technique. Samples were collected on needed basis.

Tissue and sperm extractions

Loading buffer extraction. Whole sperm extracts of spermatozoa for Western blotting were prepared by mixing washed spermatozoa (10^6 cells/ml) in loading buffer (50 mM Tris pH 6.8, 150 mM NaCl, 2% SDS, 20% glycerol, 5% β-mercaptoethanol, 0.002% bromphenol blue) and boiling for 5 min. Liver was cut into fine pieces in PBS, washed several times to remove blood and then boiled in loading buffer for 5 min. Porcine blood was centrifuged to obtain red blood cell (RBC). The pellet was washed with PBS three times to remove any plasma proteins. The cells were suspended in distilled water and frozen for several hours at -20°C. The extract was centrifuged at 16,000x g for 20 min at 4°C and the cell debris-free supernatant was collected. A small aliquot of the extract was mixed with equal volume of 2-times concentrated loading buffer. Ten microliters of extracts were loaded per lane.

Triton soluble and insoluble extraction. Freshly ejaculated boar semen samples were washed four times with warm PBS with mild centrifugation. The final pellets were suspended as a thick paste in PBS extraction buffer containing 0.1% Triton X100, 1 mM PMSF, 5 mM EDTA. The suspensions were freeze-thawed for four cycles, centrifuged three times at 16,000x g to obtain extracts as clear supernatants that were used as soluble protein fraction for Western blotting. The pellets were saved for extracting the insoluble (pellet) fraction of protein. The total protein concentration of the supernatant fractions was estimated by using Bradford reagent (www.bio-rad.com). The extracts were aliquoted and stored in -80^0C freezer until used. Sperm-free seminal plasma extracts were obtained by centrifuging semen three times. Protein concentration of the clear supernatant was estimated by the Bradford method and diluted to a required concentration with PBS extraction buffer.

For Western blotting the Triton soluble supernatant protein factions were mixed with 2-times or 1-time concentrated loading buffer. The Triton insoluble proteins contained in the pellet fractions were washed 3-times with PBS extraction buffer and boiled in loading buffer.

DTT-Triton extraction. Boar seminiferous tubules and spermatozoa were prepared as described above and extracted by the freeze-thaw method with PBS-DTT-Triton extraction buffer (PBS +1 mM DTT, 0.1% Triton1 mM PMSF and 5 mM EDTA). The seminiferous tubule extract was used for immunoprecipitation and the sperm extract was used for Western blotting and peroxidase enzymatic activity estimation.

Mouse spermatids isolation. The testicular capsules were torn apart with the help of two pointed forceps and the seminiferous tubules were released into the TL-PVP medium. The tubules were spread and washed several times in TL-Hepes to remove the intertubular stromal cells. Finally the tubules were minced with fine scissors, pipetted in-and-out several times,with Pasteur pipette and filtered through 50 μm nylon mesh. Small aliquots of the cell suspension were applied on poly-L-lysine coated coverslips and processed for antibody labeling.

For Western blotting experiments, mouse germ cells were isolated by an enzymatic method [23]. Blood vessels and blood were carefully removed before and after releasing the seminiferous tubules from the testis capsule.

SDS PAGE and Western blotting

Electrophoresis was done on 4-20% Tris-glycine gradient gels (PAGEr, www.lonza.com), transferred to PVDF membrane by using wet transfer system [24]. Tris-buffered saline (pH 7.4) with 0.1% Tween-20 (TBS-Tween) was used for washing membranes and incubating with antibody. The PVDF membranes were blocked with 10% non-fat milk, incubated with PRDX2 antibody (2 microlitres in 10 ml of TBS-Tween with 1% non-fat milk; antibody stock ,1 mg/ml) overnight at 4°C, then with HRP conjugated secondary antibody (10,000-times dilution) at room temperature for 1 h, processed with chemiluminiscent reagent by using a commercial kit (Immobilon, www.millipore.com) and visualized by exposure to X-ray film.

For reprobing, the PVDF membranes were washed with stripping buffer containing Tris-buffer (50 mM, pH 6.8), SDS (1%) and betamercaptoethanol (100 mM) by rocking for 15 min at 40°C. The membranes were washed 4-times with TBS-Tween, blocked with 10% nonfat milk and incubated with anti β-tubulin antibody (E7, 2,000-times dilution). Washing, incubation with secondary antibody and development were done as described above.

Control Western blotting was done by using immunoadsorbed antibody. Two micrograms of anti PRDX2 antibody (1E8) was incubated with 3 micrograms of human recombinant PRDX2 protein (protein stock, 1 mg/ml) in 10 ml of TBS-Tween with 1% nonfat milk for 1 h. The neutralized antibody solution was used for Western blotting various extracts by following the standard protocol.

Immunoprecipitation

Immunoprecipitation of boar seminiferous tubule extract was done with PRDX2 antibody. Four hundred microliters of DTT-Triton extract was precleaned by mixing with 30 µl of protein-G agarose beads (Immobilized protein-G plus, www.piercenet.com) and slowly rocked for 1 h at room temperature. The extracts were retrieved and mixed with 3 µl anti-PRDX2 antibody and rocked at room temperature for 1 h with slow rocking. Thirty microliter of protein-G agarose beads was added to the mixture and rocked for an additional hour. Antibody control was prepared by mixing 3 µl of antibody with 400 µl of PBS extraction buffer and incubating with 30 µl of protein-G agarose beads. After incubation, the beads were washed 4 times with PBS extraction buffer and finally boiled with 30 µl of 2-times concentrate loading buffer.

Mass spectrometry
Coomassie stained immunoprecipitated PAGE bands were individually excised, dehydrated, reduced with DTT, alkylated with iodoacetamide, trypsinized and lyophilized by following the standard protocol (proteomics.missouri.edu/). The dried samples were reconstituted with water/formic acid (990/10 v/v) and desalted with C18 micro-Ziptips.

For MALDI TOF analysis, the extracts were loaded with alpha-cyano-4hydroxycinnamic acid matrix and loaded on stainless steel target. The MS spectra were acquired by Voyager DEPro MALDI TOF MS (www.appliedbiosystems.com) with 337 nm nitrogen laser, delayed-extraction and reflector mode. The MS spectra were acquired over the mass range of 600-6000 Da. The mass spectrum for the sample was recalibrated internally using masses of trypsin autolysis peptides, in addition to using Applied Biosystem's default calibration system. Spectra were processed with 'Data Explorer (Vers 4.0.0.00)' software.

Nanospray quadruple time of flight mass spectrometry (QqTOF MS) was performed on an Applied Biosystems/MDS Sciex (www.appliedbiosystems.com) QStar/Pulsar/i instrument fitted with a Proxeon (Odense, Denmark) nanospray source. A borosilicate glass sample capillary was used to introduce the sample into the mass spectrometer. A stable spray was achieved at 800 V in the presence of nitrogen curtain gas. The settings for the Declustering Potential (25), Focusing Potential (100), Declustering Potential 2 (15), and CAD gas (3) were kept low to minimize in-source fragmentation of peptides during MS analyses. Positive ion spectra (1 second accumulation time/spectrum) were acquired in the profile MCA mode over the mass range 425-2000 Da. Spectra were summed for at least 1 minute. A pulser frequency of 6.99 KHz was used for both the MS and MS/MS mass ranges. External calibration of the instrument was based on MS/MS fragment ions from [Glu^1]-Fibrinopeptide B obtained with nitrogen collision gas (setting of 6) and a collision energy of 40 (the potential difference between the front-end RF-only quadrupole (Q0) and the collision cell (Q2). The MS/MS for the sample peptides were obtained with collision energies which produced an even distribution of fragment ions across the mass range (50-2000 Da). The resolution of the precursor ion mass window was adjusted as needed to minimize interference from background. The instrument software was Analyst QS and the data analysis software was BioAnalyst 1.1.

The MS/MS spectra were centroided (merge distance 100 ppm; percentage height ≤S0.01 %; minimum width 10 ppm; maximum width 50 ppm), and the data was submitted via BioAnalyst software to the public website for Matrix Science's Mascot "MS/MS Ion Search" program (www.matrixscience.com). Searches were performed against the NCBInr Mammalian or "other Mammals" protein databases.

Immunofluorescence labeling
Diluted spermatozoa were applied to poly-L-lysine coated coverslips, fixed with 2% formaldehyde in PBS and permeabilized with 0.1% Triton X-100 (1 h). The cells were sequentially incubated with 5% normal goat serum (blocking), first antibody (50-times diluted), fluorochrome-conjugated (mostly TRITC) secondary antibody (80-times dilution), DAPI (5 μg/ml) and mounted on microscopy slides in a small drop of VectaShield medium (www.vectorlabs.com). Testicular germ cells were isolated as described above, and processed in a similar way as the spermatozoa. Multiplex labeling with E7 (anti β-tubulin antibody) or FITC-conjugated peanut agglutinin (acrosome labeling) was done after completing labeling with the first set of antibodies, but before DAPI labeling.

Control labelings were done with preneutralized antibody. Two microliters PRDX2 antibody was mixed with 3 µl of human recombinant PRDX2 protein in 100 µl of PBS and kept at room

temperature for 1 h. The mixture was used for labeling boar and mouse spermatozoa by following the standard method, described above.

NADPH oxidation activity assay

Peroxidase enzyme reactions of the sperm extracts and seminal plasma were carried out in 2 ml Eppendorf tubes. Before starting reaction, 1 ml of pre-reaction mixture A (PRM-A) was prepared containing 200 µg/ml extracts and 100 µM H_2O_2 in tubes by adjusting the concentration with Hepes buffer (50 mM, pH 7.0). Pre-reaction mixture B (PRM-B) was prepared separately comprised of 2 mM EDTA and 400 µM NADPH in Hepes buffer (stock solution 6 mM NADPH, stored in -80°C until used). The reaction was started by adding 1 ml of PRM-B into the PRM-A. The final 2 ml of complete reaction mixture comprised of extract-100 µg/ml; H_2O_2- 50 µM; and NADPH- 200 µM. The reaction was allowed to proceed for 5 min at room temperature. The entire reaction mixture of each assay point was dispensed into 10 wells of 96-well plate, 200 µl in each well and absorbance was read at 340 nm with a Biotek EL 808 Ultramicroplate Reader (www.biotek.com). Control samples comprised mixture of PRM-A and PRM-B prepared as described above but without H_2O_2 in the PRM-A. The difference in NADPH content observed in between the control and the reaction samples after 5 min incubation was considered as the amount of NADPH lost due to peroxidase activity. The effects of carmustin and diethyl maleate were investigated by mixing these drugs with the extracts, vortexing briefly and incubating for 10 min before adding H_2O_2 and PRM-B.

The assays were performed in 3 samples from 3 boars. Each assay point is presented as a mean value, comprising 10 replicate readings. The mean and standard deviations were calculated using MS-Excel spreadsheet. The data were subjected to one-way analysis of variance (ANOVA) from the website www.physics.csbsju.edu/stats/, followed by Student's T-test using MS- Excel spreadsheet.

Results

The PRDX2 antibody recognizes a 20 kDa band in mammalian spermatozoa and spermatid extracts

Western blotting of boar and mouse spermatozoa with anti-PRDX2 monoclonal antibody (mAb 1E8) revealed a distinct 20 kDa band (Fig. 1A). Boar spermatozoa also displayed a 60 kDa diffuse band in addition to the 20 kDa band while boar testicular tissue extracts displayed a strong 20 kDa band. Sperm-free boar seminal plasma extracts displayed a 20 kDa band along with distinct bands at 15, 35, and 60 kDa. Porcine red blood cells (RBC), and liver extracts were included in the Western blotting experiments as positive control that exhibited a consistent PRDX2 reaction at 20 kDa (Fig. 1A). Liver extracts produced an additional band at 80 kDa.

The specificity of anti-PRDX2 ab (1E8) recognizing PRDX2 was confirmed by performing a control Western blotting experiment in which the antibody was pre-neutralized by incubating with pure recombinant human PRDX2 protein. The immunodepleted antibody did not react with the putative 20 kDa PRXD2 band in any of the boar sperm, seminiferous tubule, seminal plasma, liver or RBC extract lanes. Two weak inconspicuous bands were observed at 25 kDa and 60 kDa in the sperm lane and at 25 kDa and 80 kDa in the liver lane, while a faint band was present at 12 kDa in the seminal plasma lane (Fig. 1B).

The 20 kDa band of Sperm extract is PRDX2

To directly identify the species of PRDX present in spermatozoa and to identify its interacting proteins, boar seminiferous tubule extracts were immunoprecipitated with PRDX2 antibody, resolved by PAGE and stained with Coomassie blue. The immunoprecipitated extract exhibited a diffuse band in the 20-23 kDa range along with an additional band of 18 kDa (Fig. 2).

MALDI TOF/MS analysis of the 20-23 kDa band of the immunoprecipitated extract revealed two $[M+H]^+$ ions at m/z 1070.54 and 1211.71 Da that were assigned to porcine PRDX2 (<30 ppm error). Further analysis revealed a $[M+H]^{2+}$ ion at 606.36 Da matching with the derivative of the $[M+H]^+$ ion of 1211.71 Da. Microsequencing by nanospray QqTOF MS/MS revealed a peptide fragment QITVNDLPVGR that matched with porcine PRDX2 [aa, 101-111]. The $[M+H]^{2+}$ ion at m/z 606.36 Da was contaminated by $[M+H]^{3+}$ ion that was found to be trypsin ion by *de novo* sequencing. Analysis of the 535.8 Da $[M+H]^{2+}$ ion, a possible derivative of the 1070.54 Da $[M+H]^+$ ion, resulted in a non-matching sequence (unknown, gi:62988875) with PRDX2. Five other prominent ions were also analyzed by nanospray QqTOF MS/MS, four of which were found to be sperm mitochondrion associated cysteine-rich protein (SMCP) and one ion was glutathione peroxidase-4 (Table 1). The 18 kDa band of the immunoprecipitated extract was analyzed by 4700 MALDI TOF MS/MS. Three prominent ions were found to match cellular nuclear binding protein (CNBP) and four ions matched glutathione peroxidase-4 (Table 2).

Testicular PRDX2 is soluble but sperm PRDX2 is insoluble

The supernatant and pellet fractions of the freeze-thaw extracts of boar seminiferous tubule cells and spermatozoa were analyzed by Western blotting. The PRDX2 band was observed only in the Triton-soluble (supernatant) fraction of the testicular cells; the insoluble pellet fraction lacked detectable bands (Fig. 3A). Re-blotting the PVDF membranes with anti-β-tubulin antibody revealed a larger band in the pellet lane than in the supernatant lane (Fig. 3B). In spermatozoa, PRDX2 band was observed in the insoluble pellet fraction; the Triton-soluble supernatant fraction did not contain detectable bands. Remarkably, the Triton insoluble PRDX2 of spermatozoa was a 60 kDa band as compared to the 20 kDa band of the Triton soluble spermatid PRDX2. The pellet fraction of sperm extract possessed β-tubulin band whereas the supernatant extract lacked this band (Fig. 3B). The RBC lane showed the characteristic PRDX2 band but lacked β-tubulin. Boar spermatozoa were further extracted with PBS extraction buffer containing DTT-Triton and analyzed by Western blotting. DTT-Triton extraction revealed the PRDX2 bands at 60 kDa and 20 kDa (Fig. 3C).

Similar to boar spermatids, PRDX2 band was observed only in the Triton soluble fraction of the seminiferous tubule cell extracts of mice, but not in the insoluble pellet fraction. The β-tubulin labeling in both lanes was approximately equal (Supplemental Fig. S1 and all Supplemental Figures are available online at www.biolreprod.org).

Besides performing β-tubulin blot as a loading control, the protein load in different lanes was also estimated visually by comparing the staining intensities of the residual protein bands in the Coomassie blue stained PAGE after protein transferred to a PVDF membrane. Staining intensities of the residual protein bands in the transferred PAGE were approximately equal in the boar testicular cells and spermatozoa lanes of the supernatant and pellet fractions (Supplemental Fig. S2) indicating comparatively equal protein loads in those lanes. The PVDF membranes were stained with Ponceau S stain after β-tubulin blotting that also revealed comparatively equal protein load in the individual lanes (data not shown).

PRDX2 is localized in the cytoplasm of spermatids and in the post-acrosomal sheath of sperm heads

In mouse spermatocytes and spermatids, PRDX2 exhibited a diffuse labeling pattern in the cytoplasm, excluded from the nuclear area (Fig. 4A-C). In the late step elongating spermatids, the labeling was observed in the cytoplasmic lobes (Fig. 4D-E) that were eventually discarded as residual bodies. PRDX2 labeling was observed mainly in the mitochondrial sheath and in the cytoplasmic droplets of the late stage spermatids (Fig. 4F-G). In cauda epididymal

spermatozoa, PRDX2 labeling was observed in the mid-piece region (Fig. 4H). Some spermatozoa also expressed PRDX2 in the post-acrosomal sheath region (Fig. 4H, Inset).

Similar localization was also observed in boar spermatozoa (Fig. 4I). Some spermatozoa that have undergone spontaneous acrosome reaction, expressed PRDX2 in the post-acrosomal region (Fig. 4I, Inset). Control labeling of boar and mouse spermatozoa done by incubating with immunoadsorbed (neutralized), PRDX2 antibody did not reveal any detectable labeling (Supplemental Fig. S3).

Boar sperm extracts oxidize NADPH in the presence of H_2O_2

Peroxidase enzymatic activity of boar sperm redox proteins was assayed by evaluating the rate of NADPH oxidation after adding hydrogen peroxide and NADPH in the reaction mixture containing sperm extracts. Oxidation of NADPH in the reaction system was evaluated by measuring changes in the absorbance values at 340 nm. The optimum oxidation of NADPH was observed at 50 µM concentration of H_2O_2 (Fig. 5A). The reaction rate dropped sharply at higher concentrations of H_2O_2. The NADPH oxidation rate was similar to the control value when H_2O_2 concentration was 150 µM or higher. The rate of the reaction increased exponentially from 0 to 10 min after mixing the extract with H_2O_2 and NADPH (Fig. 5B). Hence, the 5 min time-point was considered as half of the time required to reach maximum reaction velocity ($½V_{max}$). The reaction rates were estimated at 5 min after the start of the reaction in subsequent experiments. The rate of reaction also increased exponentially with the increase in sperm extract concentration up to 100 µg/ml total protein. It remained nearly constant with further increase in extract concentration (Fig. 5C). At 100 µg/ml of protein concentration, NADPH oxidation rate was 20 µM/5 min. In the subsequent experiments, concentrations of NADPH, H_2O_2 and extract were 200 µM, 50 µM and 100 µg/ml, respectively. NADPH was not oxidized by H_2O_2 alone (without including the sperm extract) or by sperm extract alone (without H_2O_2).

The sperm-free seminal plasma fraction of the boar semen also showed peroxidase enzyme activity. Similar to sperm extract, the reaction rate of NADPH oxidation increased exponentially with the increase of seminal plasma concentration up to100 µg/ml of total protein (Fig. 5D). The reaction rate remained nearly constant with further increase in the seminal plasma concentration. At 100 µg/ml of protein concentration, the NADPH oxidation rate was 11 µM/5 min., i.e. approximately half the rate observed in sperm extracts.

Diethyl maleate reduces the NADPH oxidizing activity of sperm extract while carmustin (BCNU) shows no effect

Diethyl maleate (DEM) and carmustin (BCNU) are anticancer drugs that block glutathione pathway. DEM binds irreversibly to glutathione via reaction catalyzed by glutathione-S-transferase [25] making it unavailable for redox reactions. BCNU inhibits glutathione reductase [26] thereby blocking regeneration of reduced glutathione.

To find to what extent the NADPH oxidation by sperm extract is due to glutathione and/or glutathione reductase activities, the rate of NADPH oxidation was estimated in the presence of DEM or BCNU. Addition of DEM in the reaction mixture diminished the NADPH oxidizing activity of sperm extract in a dose dependent manner. The enzyme activity was inhibited to about 50% in the presence of 70 mM DEM in the reaction mixture (Fig. 5E). Carmustin, on the other hand, did not cause significant inhibitory effect. Addition of 50 µM carmustin to the reaction mixture reduced the enzyme activity to about 10% (Fig. 5F). Further decrease in the reaction rate was not observed by increasing the inhibitor concentration.

The biological activity of carmustin was evaluated by assessing its effect on porcine *in vitro* oocyte maturation system. The drug inhibited cumulus expansion and nuclear maturation of the oocytes at physiological concentrations (Supplemental Table S1).

Discussion

The present study demonstrates that mammalian spermatozoa and seminal plasma possess PRDX2 protein. The sperm redox system is functionally active and potentially plays an important role in protecting spermatozoa from reactive oxygen species in the female reproductive milieu until fertilization in ensured. Inhibition of glutathione system only partially obstructs the peroxidase enzyme activity of the sperm extract.

Peroxiredoxin 2 is Present in Mammalian Spermatids and Spermatozoa

The observation of a 20 kDa band in Western blotting with a monoclonal anti-PRDX2 antibody provides a strong evidence for the presence of PRDX2 in mouse and boar male gametes and in boar seminal plasma. The putative 20 kDa PRDX2 was also observed in Western blotting of human and opossum sperm extracts (data not shown). The specificity of the antibody to recognize 20 kDa PRDX2 band was verified by performing a control Western blotting. When the antibody was preadsorbed with human recombinant PRDX2 protein, its reaction at the 20 kDa band was completely eliminated. However, such blotting experiments revealed very faint bands at 12, 25, 60 or 80 kDa, possibly due to contamination of unrelated antibody. Nevertheless, the residual reaction of the preadsorbed antibody was negligible in comparison to the native antibody. The specificity of the antibody to PRDX2 was further verified by running RBC and liver extracts as positive control lanes in Western blotting experiments. Purified PRDX2 (calpromotin) from RBC exhibits the characteristic 20 kDa band in SDS Western blotting [15, 27]. The anti-PRDX2 antibody also reacted with a 20 kDa band in liver cells extracts. Immunoprecipitation of boar testicular cell extracts with PRDX2 antibody pulled out a putative PRDX2 band and nanospray MS/MS sequencing of the band extract revealed the presence of PRDX2 ions, conferring a strong evidence for the presence of PRDX2 in the boar male gametes.

Peroxideroxin 2 is a Moonlighting Protein in Spermatids and Spermatozoa

Western blotting experiments further revealed that the PRDX2 of the differentiating spermatids is mostly soluble while that of mature spermatozoa is insoluble. Triton insoluble PRDX2 of boar spermatozoa appeared as a 60 kDa band that was also observed when the whole spermatozoa were extracted by PAGE loading buffer. When the spermatozoa were rigorously extracted with DTT-Triton, a 20 kDa band was expressed along with the 60 kDa band. These observations further support a possibility that the 60 kDa band of boar and bull spermatozoa is an oligomerized or covalently conjugated PRDX2 [10] that is resilient to extraction by Triton. A 60 kDa PRDX2 band was also observed in bull sperm extracts (data not shown).

These data suggest that PRDX2 is a ‘moonlighting protein’ that may have multiple functions. The soluble PRDX2 in spermatids is diffusely localized in the spermatid cytoplasm, most of which is discarded with the residual bodies during spermiation. The soluble PRDX2 is likely to be enzymatically active and may protect cells from peroxidative damage. During the late spermiogenesis stage the PRDX2 is processed into an insoluble form and associated with the mitochondrial sheath. It was also observed in the post-acrosomal region of the perinuclear theca which comprises mostly condensed cytosolic proteins that are structurally rigid and highly resistant to extraction [28]. Functional transformation is displayed by other members of PRDX family occurring in spermatozoa. PRDX4 is initially synthesized as a membrane binding 31 kDa protein in rat spermatids, possibly involved in acrosome biogenesis [21]. After maturity, the PRDX4 is processed into a 27 kDa secretory form and discarded with the residual bodies.

PRDX5 is constitutively a mitochondrial protein but was also detected in the isolated boar sperm acrosomal membrane fractions that interacted with the zona pellucida during fertilization [22].

The Cementing Material of the Sperm Mitochondrial Sheath is a Complex of Condensed Cysteine-rich Proteins

Immunoprecipitation with PRDX2 antibody pulled out three other proteins namely, GPX4, sperm mitochondrion-associated cysteine-rich protein (SMCP) and cellular nucleic acid binding protein (CNBP) along with PRDX2 itself. Among them GPX4 and SMCP are known to be multifunctional proteins responsible for the structural integrity of the mitochondrial sheath in mature spermatozoa. Biochemical affinity of PRDX2 to GPX4, SMCP and their colocalization in the mitochondrial sheath strongly suggests that these three proteins might functionally interact to form the mitochondrial sheath.

GPX4 is a proline- and cysteine-rich selenoprotein also referred to as the phospholipid hydroperoxide glutathione peroxidase (PHGPX). It is the most abundant sperm mitochondrial sheath protein comprising about 50% of the mitochondrial capsule material. The GPX4 is a well characterized moonlighting protein occurring in spermatids [29]. It changes its physical characteristics, subcellular localization and biological functions during spermiogenesis [30, 31]. In spermatids, GPX4 exists as a soluble and enzymatically active form, protecting cells from peroxidation. After spermatid differentiation, its enzymatic activity is lost, the protein is subsequently processed into an insoluble glue-like substance by oxidative cross linking and deposited on the outer membrane of mitochondria of the midpiece region. Similar to GPX4, PRDX2 also exists as a soluble form in immature spermatids, condenses into insoluble form after spermatid maturation and is localized in the mitochondrial sheath.

Another protein co-immunoprecipitated with PRDX2 was SMCP which is also known to be a major structural protein of the mitochondrial capsule. It is synthesized in the mid-stage spermatids, initially as a soluble cytosolic form, but later becomes deposited as an insoluble matrix on the outer mitochondrial membrane after the mitochondrial sheath is assembled [32]. The function of the nascent (soluble) form of SMCP in spermatids is not known, whereas its condensed form in mature spermatozoa is important for maintaining the integrity of the mitochondrial sheath and sperm motility [33, 34]. Previous studies have shown colocalization of SMCP with GPX4 [34].

MS/MS sequencing of the 18 kDa band of immunoprecipitated extract revealed three ions originating from cellular nucleic acid binding protein (CNBP). Unlike PRDX2, GPX4 or SMCP, CNBP is mostly a nuclear protein that binds to the CT element of *MYC* gene [35] and plays an important role in regulating embryonic gene expression [36]. Structural association between GPX4 and CNBP is possible because GPX4 also localizes in the spermatid nuclei, regulating oxidative cross-linking of protamines and ensuring proper chromatin condensation [6].

Peroxidase Activity of Sperm Extract

The function of PRDX2 in spermatozoa is speculative. As discussed above, it might play a role in stabilizing the mid-piece mitochondrial sheath and the postacrosomal sheath of perinuclear theca. Sperm PRDX2 is likely involved in the antioxidant defense system. Boar sperm and seminal plasma extracts oxidize NADPH in the presence of H_2O_2. Loss of NADPH in the presence of H_2O_2 in the reaction mixture is considered a measure of glutathione reductase activity [37] or thioredoxin reductase activity [9]. The present study has shown that the peroxidase enzymatic activity of the sperm extract was inhibited only partially by DEM while carmustin did not show noticeable effect. These results suggest that glutathione and gluthione reductase are only partially involved in NADPH oxidation in the sperm extract. Consistently, it

has been shown that rat spermatozoa are devoid of glutathione [38] or present in very small amounts [39]. The lack of glutathione in spermatozoa is possibly compensated for by protein associated thiols [40]. It is possible that spermatozoa may be able to utilize alternative sources of thiols other than glutathione [41].

Due to low profile of the glutathione system, the thioredoxin-peroxiredoxin- system might function as the major pathway in eliminating reactive oxygen in mammalian sperm. In the redox cascade H_2O_2 is neutralized by PRDX2. The oxidized PRDX2 is reduced by thioredoxin which in turn is then reduced by NADPH in the presence of thioredoxin reductase [19] (Fig. 6A). PRDX family members do not accept electron from glutathione [16] hence, the glutathione system may not be involved in regenerating native PRDX2.

Glutathione reductase and thioredoxin reductase are closely related enzymes [reviewed in 42] and the mechanisms of their activity are also similar [43]. In addition, a chimeric enzyme thioredoxin/glutathione reductase (TGR) has been identified, which is a fusion of an N-terminal glutaredoxin domain and the thioredoxin reductase module [44]. Therefore, it was assumed that the glutathione reductase inhibitor, carmustin, might also inhibit thioredoxin reductase [42]. Surprisingly, the present study demonstrated insignificant effect of carmustin on the enzyme activity of boar sperm extracts, suggesting a possibility that the inhibitor did not affect sperm thioredoxin reductase. The lack of inhibiting effect is not due to the source of the drug, handling or inappropriate experimental protocol. Carmustin used in the present experiment was found to be fully effective in obstructing cumulus expansion and oocyte nuclear maturation at very low concentrations. There is also a possibility of an alternative pathway of PRDX2 regeneration in mammalian spermatozoa, circumventing the thioredoxin system (Fig. 6B). It is not yet known whether mature spermatozoa or seminal plasma possess thioredoxin reductase or whether their sperm thioredoxin system is functional. Mouse testis shows high expression of thioredoxin reductase [44], but the recombinant sperm-specific thioredoxin-2 [45] and spermatid-specific thioredoxin-3 [18] were found to be functionally inactive *in vitro*. Further studies are needed to clearify this question.

Since seminal plasma possesses PRDX2, a possibility cannot be excluded that the sperm peroxidase activity might be due to seminal PRXD2 adsorbed on the sperm surface. The sperm extracts were washed with PBS before extraction which should eliminate the most of such contamination. Moreover PRDX2 was observed in the postacrosomal region of the permeablized spermatozoa by immunocytochemistry and in the insoluble pellet fraction by Western blotting. These observations suggest that spermatozoa retain some PRDX2 that they have synthesized during spermatid stage. Nevertheless, conclusion about the presence of PRDX2 in spermatozoa is still valid even if they fortuitously adsorb some seminal plasma PRDX2.

In summary, the present study has revealed the presence of peroxiredoxin 2 in mammalian spermatozoa and spermatids. It interacts with glutathione peroxidase 4, sperm mitochondria associated cysteine-rich protein cellular nucleic acid binding protein, and colocalizes with them in the mitochondrial sheath, possibly involving in the formation of keratinous intermitochondrial glue. The study further demonstrated peroxidase activity of the sperm extracts possibly originating from the PRDX2 and other peroxiredoxins.

Acknowledgements
We are thankful to Beverly DaGue of the Charles Gehrke Proteomics Center of MU for mass spectrometric analysis. August Rieke collected boar semen, David Wax and Lee Spate helped collecting porcine ovaries. Kathy Craighead assisted by administrative support and proof-

reading the manuscript. This work was in part funded by the Food for the 21st Century Program of The University of Missouri and by the National Research Initiative Competitive Grant No. 2007-01319 from the USDA CSREES to P.S.

References

1. Wang X, Sharma RK, Sikka SC, Thomas AJ, Jr., Falcone T, Agarwal A. Oxidative stress is associated with increased apoptosis leading to spermatozoa DNA damage in patients with male factor infertility. Fertil Steril 2003; 80: 531-535.
2. Pasqualotto FF, Sharma RK, Nelson DR, Thomas AJ, Agarwal A. Relationship between oxidative stress, semen characteristics, and clinical diagnosis in men undergoing infertility investigation. Fertil Steril 2000; 73: 459-464.
3. Rhee SG. Cell signaling. H2O2, a necessary evil for cell signaling. Science 2006; 312: 1882-1883.
4. de Lamirande E, Gagnon C. A positive role for the superoxide anion in triggering hyperactivation and capacitation of human spermatozoa. Int J Androl 1993; 16: 21-25.
5. Aitken RJ, Paterson M, Fisher H, Buckingham DW, van Duin M. Redox regulation of tyrosine phosphorylation in human spermatozoa and its role in the control of human sperm function. J Cell Sci 1995; 108 (Pt 5): 2017-2025.
6. Pfeifer H, Conrad M, Roethlein D, Kyriakopoulos A, Brielmeier M, Bornkamm GW, Behne D. Identification of a specific sperm nuclei selenoenzyme necessary for protamine thiol cross-linking during sperm maturation. Faseb J 2001; 15: 1236-1238.
7. Cassani P, Beconi MT, O'Flaherty C. Relationship between total superoxide dismutase activity with lipid peroxidation, dynamics and morphological parameters in canine semen. Anim Reprod Sci 2005; 86: 163-173.
8. Kawakami E, Takemura A, Sakuma M, Takano M, Hirano T, Hori T, Tsutsui T. Superoxide dismutase and catalase activities in the seminal plasma of normozoospermic and asthenozoospermic Beagles. J Vet Med Sci 2007; 69: 133-136.
9. Arner ES, Holmgren A. Physiological functions of thioredoxin and thioredoxin reductase. Eur J Biochem 2000; 267: 6102-6109.
10. Wood ZA, Schroder E, Robin Harris J, Poole LB. Structure, mechanism and regulation of peroxiredoxins. Trends Biochem Sci 2003; 28: 32-40.
11. Jimenez A, Zu W, Rawe VY, Pelto-Huikko M, Flickinger CJ, Sutovsky P, Gustafsson JA, Oko R, Miranda-Vizuete A. Spermatocyte/spermatid-specific thioredoxin-3, a novel Golgi apparatus-associated thioredoxin, is a specific marker of aberrant spermatogenesis. J Biol Chem 2004; 279: 34971-34982.
12. Miranda-Vizuete A, Sadek CM, Jimenez A, Krause WJ, Sutovsky P, Oko R. The mammalian testis-specific thioredoxin system. Antioxid Redox Signal 2004; 6: 25-40.
13. Wood ZA, Poole LB, Karplus PA. Peroxiredoxin evolution and the regulation of hydrogen peroxide signaling. Science 2003; 300: 650-653.
14. Leyens G, Donnay I, Knoops B. Cloning of bovine peroxiredoxins-gene expression in bovine tissues and amino acid sequence comparison with rat, mouse and primate peroxiredoxins. Comp Biochem Physiol B Biochem Mol Biol 2003; 136: 943-955.
15. Moore RB, Mankad MV, Shriver SK, Mankad VN, Plishker GA. Reconstitution of Ca(2+)-dependent K+ transport in erythrocyte membrane vesicles requires a cytoplasmic protein. J Biol Chem 1991; 266: 18964-18968.
16. Chae HZ, Kim HJ, Kang SW, Rhee SG. Characterization of three isoforms of mammalian peroxiredoxin that reduce peroxides in the presence of thioredoxin. Diabetes Res Clin Pract 1999; 45: 101-112.
17. Chevallet M, Wagner E, Luche S, van Dorsselaer A, Leize-Wagner E, Rabilloud T. Regeneration of peroxiredoxins during recovery after oxidative stress: only some overoxidized

peroxiredoxins can be reduced during recovery after oxidative stress. J Biol Chem 2003; 278: 37146-37153.
18. Peskin AV, Low FM, Paton LN, Maghzal GJ, Hampton MB, Winterbourn CC. The high reactivity of peroxiredoxin 2 with H_2O_2 is not reflected in its reaction with other oxidants and thiol reagents. J Biol Chem 2007; 282: 11885-11892.
19. Berggren MI, Husbeck B, Samulitis B, Baker AF, Gallegos A, Powis G. Thioredoxin peroxidase-1 (peroxiredoxin-1) is increased in thioredoxin-1 transfected cells and results in enhanced protection against apoptosis caused by hydrogen peroxide but not by other agents including dexamethasone, etoposide, and doxorubicin. Arch Biochem Biophys 2001; 392: 103-109.
20. Lee K, Park JS, Kim YJ, Soo Lee YS, Sook Hwang TS, Kim DJ, Park EM, Park YM. Differential expression of Prx I and II in mouse testis and their up-regulation by radiation. Biochem Biophys Res Commun 2002; 296: 337-342.
21. Sasagawa I, Matsuki S, Suzuki Y, Iuchi Y, Tohya K, Kimura M, Nakada T, Fujii J. Possible involvement of the membrane-bound form of peroxiredoxin 4 in acrosome formation during spermiogenesis of rats. Eur J Biochem 2001; 268: 3053-3061.
22. van Gestel RA, Brewis IA, Ashton PR, Brouwers JF, Gadella BM. Multiple proteins present in purified porcine sperm apical plasma membranes interact with the zona pellucida of the oocyte. Mol Hum Reprod 2007; 13: 445-454.
23. Bellve AR. Purification, culture, and fractionation of spermatogenic cells. Methods Enzymol 1993; 225: 84-113.
24. Towbin H, Staehelin T, Gordon J. Electrophoretic transfer of proteins from polyacrylamide gels to nitrocellulose sheets: procedure and some applications. Proc Natl Acad Sci U S A 1979; 76: 4350-4354.
25. Bizzozero OA, Ziegler JL, De Jesus G, Bolognani F. Acute depletion of reduced glutathione causes extensive carbonylation of rat brain proteins. J Neurosci Res 2006; 83: 656-667.
26. Frischer H, Ahmad T. Severe generalized glutathione reductase deficiency after antitumor chemotherapy with BCNU" [1,3-bis(chloroethyl)-1-nitrosourea]. J Lab Clin Med 1977; 89: 1080-1091.
27. Low FM, Hampton MB, Peskin AV, Winterbourn CC. Peroxiredoxin 2 functions as a noncatalytic scavenger of low-level hydrogen peroxide in the erythrocyte. Blood 2007; 109: 2611-2617.
28. Oko R, Maravei D. Protein composition of the perinuclear theca of bull spermatozoa. Biol Reprod 1994; 50: 1000-1014.
29. Haraguchi CM, Mabuchi T, Hirata S, Shoda T, Yamada AT, Hoshi K, Yokota S. Spatiotemporal changes of levels of a moonlighting protein, phospholipid hydroperoxide glutathione peroxidase, in subcellular compartments during spermatogenesis in the rat testis. Biol Reprod 2003; 69: 885-895.
30. Ursini F, Heim S, Kiess M, Maiorino M, Roveri A, Wissing J, Flohe L. Dual function of the selenoprotein PHGPx during sperm maturation. Science 1999; 285: 1393-1396.
31. Flohe L. Selenium in mammalian spermiogenesis. Biol Chem 2007; 388: 987-995.
32. Cataldo L, Baig K, Oko R, Mastrangelo MA, Kleene KC. Developmental expression, intracellular localization, and selenium content of the cysteine-rich protein associated with the mitochondrial capsules of mouse sperm. Mol Reprod Dev 1996; 45: 320-331.
33. Nayernia K, Adham IM, Burkhardt-Gottges E, Neesen J, Rieche M, Wolf S, Sancken U, Kleene K, Engel W. Asthenozoospermia in mice with targeted deletion of the sperm mitochondrion-associated cysteine-rich protein (SMCP) gene. Mol Cell Biol 2002; 22: 3046-3052.
34. Nayernia K, Diaconu M, Aumuller G, Wennemuth G, Schwandt I, Kleene K, Kuehn H, Engel W. Phospholipid hydroperoxide glutathione peroxidase: expression pattern during

testicular development in mouse and evolutionary conservation in spermatozoa. Mol Reprod Dev 2004; 67: 458-464.
35. Shimizu K, Chen W, Ashique AM, Moroi R, Li YP. Molecular cloning, developmental expression, promoter analysis and functional characterization of the mouse CNBP gene. Gene 2003; 307: 51-62.
36. Armas P, Cachero S, Lombardo VA, Weiner A, Allende ML, Calcaterra NB. Zebrafish cellular nucleic acid-binding protein: gene structure and developmental behaviour. Gene 2004; 337: 151-161.
37. Staal GE, Veeger C. The reaction mechanism of glutathione reductase from human erythrocytes. Biochim Biophys Acta 1969; 185: 49-62.
38. Bauche F, Fouchard MH, Jegou B. Antioxidant system in rat testicular cells. FEBS Lett 1994; 349: 392-396.
39. Tramer F, Caponecchia L, Sgro P, Martinelli M, Sandri G, Panfili E, Lenzi A, Gandini L. Native specific activity of glutathione peroxidase (GPx-1), phospholipid hydroperoxide glutathione peroxidase (PHGPx) and glutathione reductase (GR) does not differ between normo- and hypomotile human sperm samples. Int J Androl 2004; 27: 88-93.
40. Li TK. The glutathione and thiol content of mammalian spermatozoa and seminal plasma. Biol Reprod 1975; 12: 641-646.
41. Godeas C, Tramer F, Micali F, Roveri A, Maiorino M, Nisii C, Sandri G, Panfili E. Phospholipid hydroperoxide glutathione peroxidase (PHGPx) in rat testis nuclei is bound to chromatin. Biochem Mol Med 1996; 59: 118-124.
42. Gromer S, Schirmer RH, Becker K. The 58 kDa mouse selenoprotein is a BCNU-sensitive thioredoxin reductase. FEBS Lett 1997; 412: 318-320.
43. Sun QA, Kirnarsky L, Sherman S, Gladyshev VN. Selenoprotein oxidoreductase with specificity for thioredoxin and glutathione systems. Proc Natl Acad Sci U S A 2001; 98: 3673-3678.
44. Su D, Novoselov SV, Sun QA, Moustafa ME, Zhou Y, Oko R, Hatfield DL, Gladyshev VN. Mammalian selenoprotein thioredoxin-glutathione reductase. Roles in disulfide bond formation and sperm maturation. J Biol Chem 2005; 280: 26491-26498.
45. Sadek CM, Damdimopoulos AE, Pelto-Huikko M, Gustafsson JA, Spyrou G, Miranda-Vizuete A. Sptrx-2, a fusion protein composed of one thioredoxin and three tandemly repeated NDP-kinase domains is expressed in human testis germ cells. Genes Cells 2001; 6: 1077-1090.

Figure Legends

Fig. 1. (**A**) Western blotting of PRDX2 of spermatozoa of various mammalian species. The antibody reacted with 20 kDa band in, mouse and boar spermatozoa. Liver and red blood cells (RBC) extracts were included as positive control that displayed a characteristic PRDX2 band of 20 kDa. Boar seminiferous tubules extract showed 20 kDa band whereas seminal plasma extract possessed multiple anti-PRDX2 reactive bands at 12, 20, 38 and 60 kDa. (**B**) Control Western blotting of various boar tissue extracts, incubated with PRDX2 antibody that was preadsorbed with PRDX2 recombinant protein. The neutralized antibody revealed inconspicuous bands at 25 kDa and 60 kDa in boar spermatozoa, 12 kDa in seminal plasma, 25 kDa and 80 kDa bands in liver extracts. Boar testis and RBC extracts did not show any reaction. The band signals were enhanced by exposing the X-ray film for 30 min.

Fig. 2. Boar seminiferous tubules extract immunoprecipitated with anti-PRDX2 antibody, resolved by PAGE and stained with Coomassie blue (lane IP). The extract showed two sharp bands (18 and 23 kDa) and a diffuse band in between (double headed arrow). The top band corresponds to the light-chain immunoglobulin (compare with the antibody lane). The diffuse band and the lower band were excised separately, extracted and analyzed by mass spectrometry.

Fig. 3. (**A**) Western blotting of the soluble and insoluble fractions of boar spermatozoa and seminiferous tubule extracts incubated with PRDX2 antibody. Triton soluble supernatant fraction of seminiferous tubules possessed the typical PRDX2 band at 20 kDa, absent from the Triton insoluble pellet. On the contrary, Triton insoluble pellet fraction of spermatozoa possessed a PRDX2 band of 60 kDa, but Triton soluble supernatant fraction lacked it. The RBC extract displayed characteristic PRDX2 band of 20 kDa. (**B**) The PVDF membrane was stripped and reblotted with anti β-tubulin antibody. A small band of β-tubulin was detectable in the Triton soluble supernatant fraction of seminiferous tubule extract but lacking in the sperm extract. Triton insoluble pellet fraction of boar seminiferous tubules and sperm extracts possessed distinct β-tubulin bands (**C**) Western blotting of DTT-Triton extract of boar spermatozoa. The extract revealed two anti-PRDX2 reactive bands at 20- and 60 kDa.

Fig. 4. PRDX2 localization in mammalian spermatozoa and differentiating spermatids. (**A**) Mouse secondary spermatocyte, (**B**) round spermatid, (**C**) early stage elongating spermatid and (**D**) mid stage elongating spermatids possessing diffuse PRDX2 labeling in the cytoplasm. (**E**) In the late stage spermatids, the excess PRDX2 is discarded with the residual bodies (arrow). (**F**) Localization of PRDX2 in the mitochondrial sheath (arrows) was clearly revealed in the late stage spermatids that had disrupted plasma membrane. (**G**) Fully formed testicular spermatozoa displaying labeling in the mid-piece and cytoplasmic droplet (arrow). (**H**) Mouse cauda epididymal spermatozoa displaying PRDX2 localization in the mid-piece of sperm tail. Inset shows a spermatozoon in which PRDX2 was observed in the post-acrosomal sheath and mid-piece regions. (**I**) Boar ejaculated spermatozoa displaying PRDX2 in the mid-piece region. Inset: spermatozoon with a disrupted acrosome showing PRDX2 labeling in the post-acrosomal region. Bars – 5 μm.

Fig. 5. Peroxidase activity of boar sperm and seminal plasma extract. (**A**) Changes in the reaction rate at various concentration of H_2O_2. A peak of maximun activity was observed at the concentration of 50 μM H_2O_2. (**B**) Kinetics of the time-dependent changes in the reaction rate. The reaction rate reached the plateau at 10 min after the start. (**C**) Changes in the rate of reaction with progressively increasing sperm extract concentration. The reaction rate increased exponentially up to 100 μg/ml of extract concentration, beyond which it reached the plateau. (**D**) Changes in the rate of reaction with increase in the seminal plasma extract concentration. The reaction rate increased exponentially up to 100 μg/ml, beyond which the rate reached the plateau. (**E, F**) Effect of diethyl maleate (**E**) and carmustin (**F**) on the peroxidase enzyme activity of boar sperm extract. The reaction rate was reduced to 50% with the addition of 70 mM diethyl maleate. Addition of 50 μM carmustin caused a 10% drop in the rate of reaction. Further inhibition was not observed with increase in the concentration of the drug. Error bars represent standard deviations. All data of the panels E-F are statistically significant ($P < 0$ .0001) as revealed by ANOVA. Columns marked with different letters are significantly different ($P < 0.05$; Student's t-test),

Fig. 6. Peroxiredoxin-thioredoxin pathway of reduction of H_2O_2. (**A**) Peroxiredoxins reduce H_2O_2 by getting oxidized in the process. The oxidized peroxiredoxins are reverted to their active reduce state by the electrons donated by NADPH via the thioredoxin system composing of thioredoxin reductase (TRXR) and thioredoxin (TRX). (**B**) In sperm extracts, addition of carmustin has very little effect on the rate of NADPH oxidation suggesting either thioredoxin reductase is not affected by the drug, or peroxiredoxin is regenerated through an alternative pathway without thioredoxin reductase and thioredoxin being involved.

Table 1. The prominent peaks of the Nanospray Qq-TOF MS/MS spectrum of the 20-23 kDa band of the anti-PRDX2 immunoprecipitated boar seminiferous tubule extract.

M/Z Analyzed	$[M+H]^{+}$ Calculated	Match	$[M+H]^{+}$ Error ($p<0.05$)	Ion Score
934.47	1867.93	K[GSQSPQSPPGAQGNWNQK]K*	27 ppm	52(>41)
974.43	1947.85	K[GSQSPQSPPGAQGNWNQK]K*	5 ppm	61(>46)
949.92	3760.66	K[TNQCPPPCCPPKPCCPPKPCCPQKPPCCPK]S*	8 ppm	4(>42)◘
666.03	1996.97	K[GSQSPQSPPGAQGNWNQKK]S*	50 ppm	22(>20)
548.98	1644.92	K[TDVNYTQLVDLHAR]Y+	49 ppm	52(>43)

*NCBInr gi: 28202255 (sMCRP); +NCBInr gi: 27807491 (GPX4); ◘Low score due to high number of multiple charge fragment ions not taken into account in the Mascot search

Table 2. 4700 MALDI-TOF MS analysis of 18 kDa band of the anti-PRDX2 immunoprecipitated boar sperm extract.

M/Z $[M+H]^+$	Calculated Peptide Mr	MS/MS Fragment	Gene Indices (gi)	Ion Score	Matches
1484.62	1484.62	CYSCGEFGHIQK	73984502*	35	26/248
1774.65	1774.63	DCDLQEDACYNCGR	73984502*	108	27/218
1848.79	1848.78	EQCCYNCGKPGHLAR	73984502*	68	27/238
867.39	868.4	YAECGLR	93215895^+	21	23/70
1321.67	1322.67	AFPCNQFGR	93215895^+	57	35/129
1643.84	1644.85	TDVNYTQLVDLHAR	93215895^+	89	39/230
1336.69		L/IAFPCNQFGR	GPX4 (aa 74-84)	*de novo* sequenced$^+$	

*Cellular nucleic acid binding protein isoform 1;
+Glutathione peroxidase 4

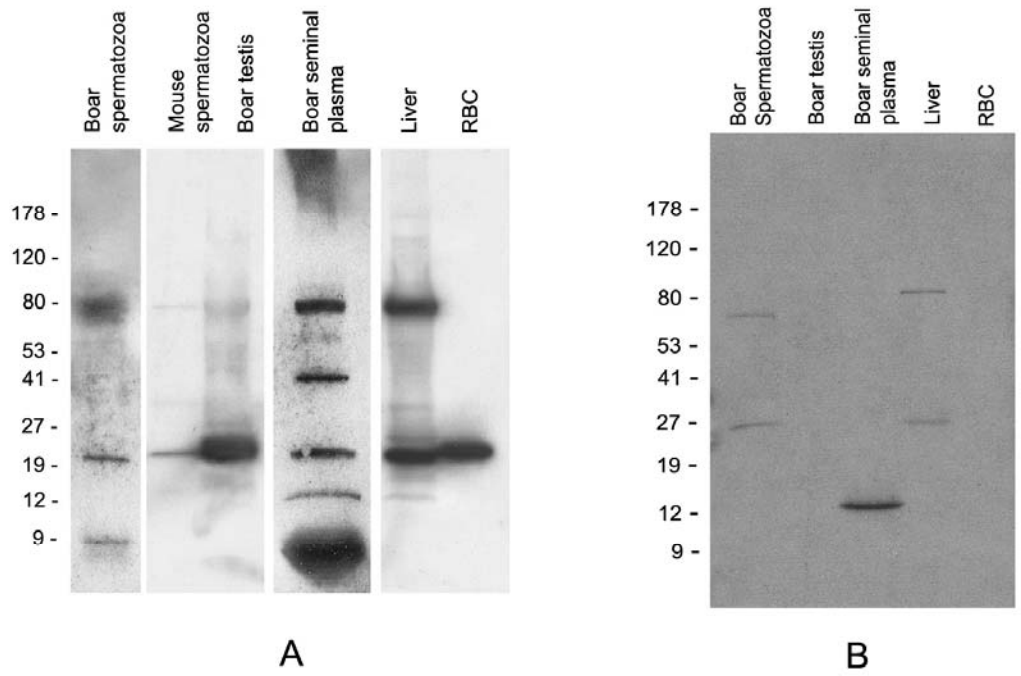
Boar spermatozoa
Mouse spermatozoa
Boar testis
Boar seminal plasma
Liver
RBC
178 -
120 -
80 -
53 -
41 -
27 -
19 -
12 -
9 -
A
Boar Spermatozoa
Boar testis
Boar seminal plasma
Liver
RBC
178 -
120 -
80 -
53 -
41 -
27 -
19 -
12 -
9 -
B

Fig. 1.

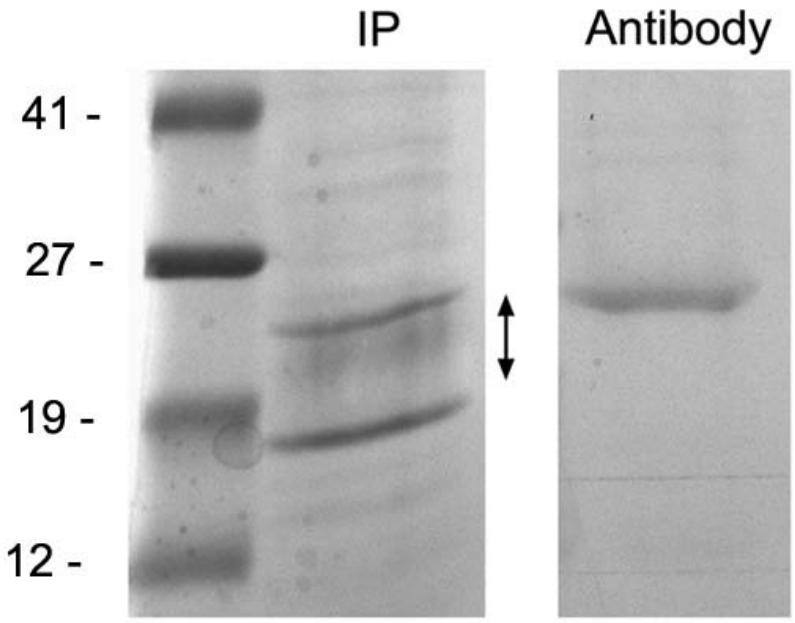

Fig. 2

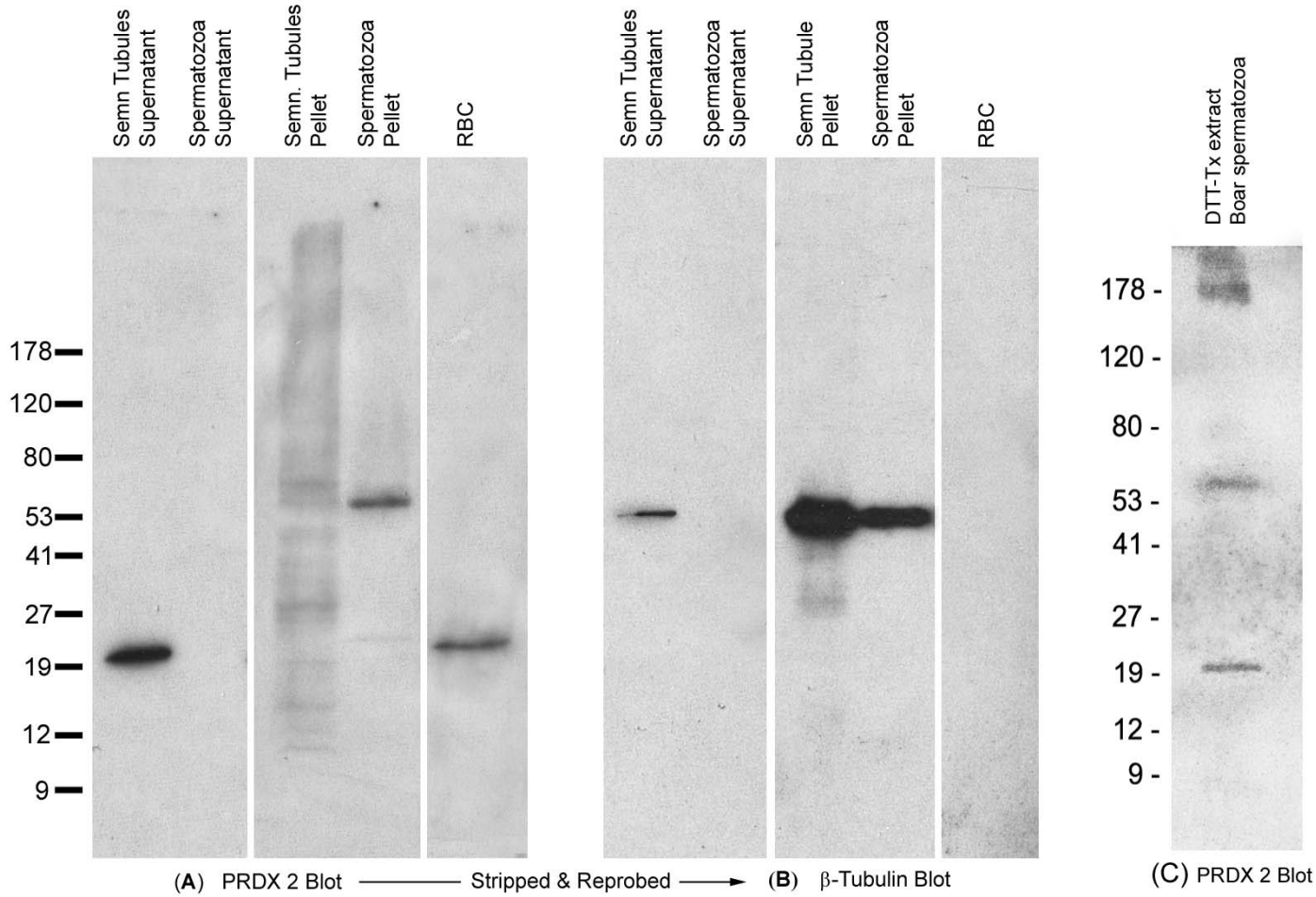
Semn Tubules Supernatant
Spermatozoa Supernatant
Semn. Tubules Pellet
Spermatozoa Pellet
RBC
178
120
80
53
41
27
19
12
9
(A) PRDX 2 Blot
Stripped & Reprobed
(B) β-Tubulin Blot
Semn Tubules Supernatant
Spermatozoa Supernatant
Semn Tubule Pellet
Spermatozoa Pellet
RBC
DTT-Tx extract Boar spermatozoa
178 -
120 -
80 -
53 -
41 -
27 -
19 -
12 -
9 -
(C) PRDX 2 Blot

Fig. 3

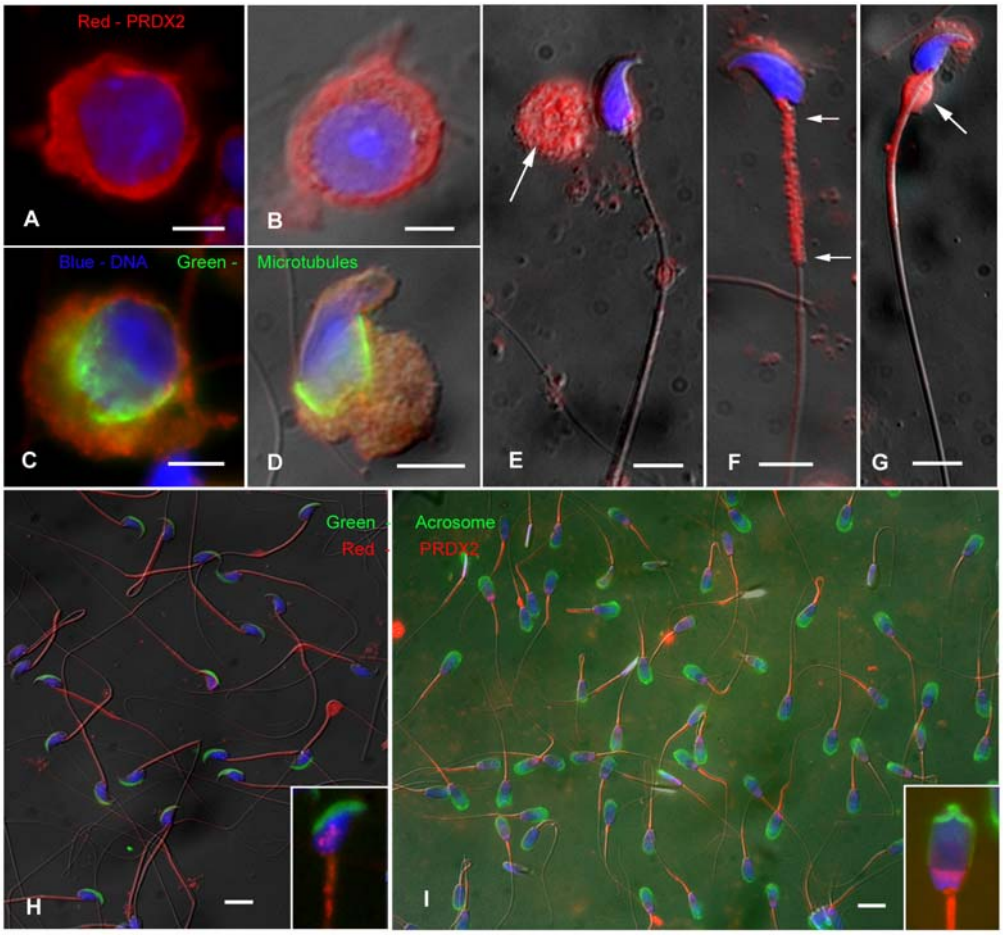
Red - PRDX2
A
B
Blue - DNA
Green -
C
Microtubules
D
E
F
G
Green -
Red -
H
Acrosome
PRDX2
I

Fig. 4.

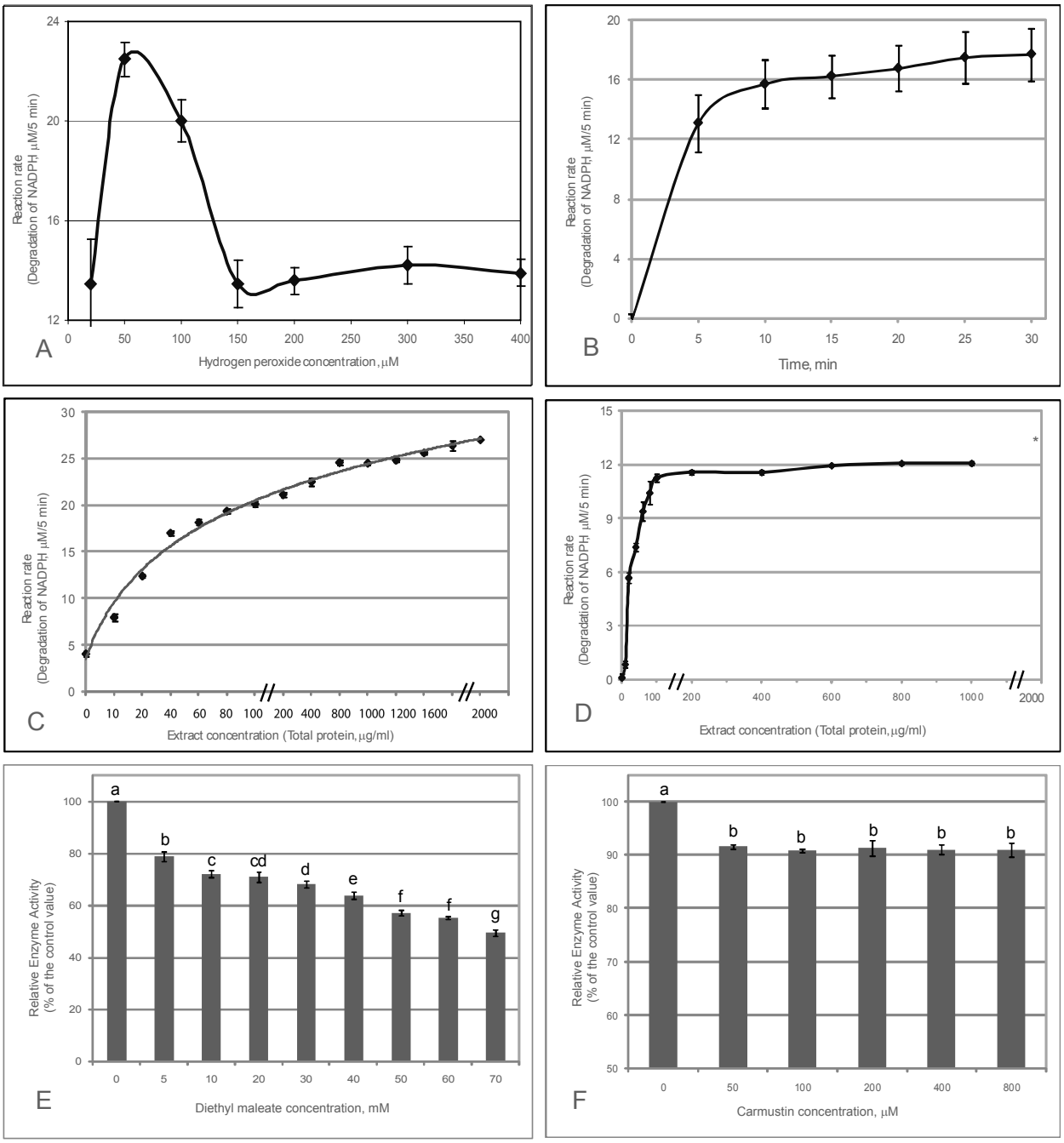
A
Reaction rate (Degradation of NADPH μM/5 min)
Hydrogen peroxide concentration, μM
B
Reaction rate (Degradation of NADPH μM/5 min)
Time, min
C
Reaction rate (Degradation of NADPH μM/5 min)
Extract concentration (Total protein, μg/ml)
D
Reaction rate (Degradation of NADPH μM/5 min)
Extract concentration (Total protein, μg/ml)
E
Relative Enzyme Activity (% of the control value)
Diethyl maleate concentration, mM
F
Relative Enzyme Activity (% of the control value)
Carmustin concentration, μM

Fig. 5.

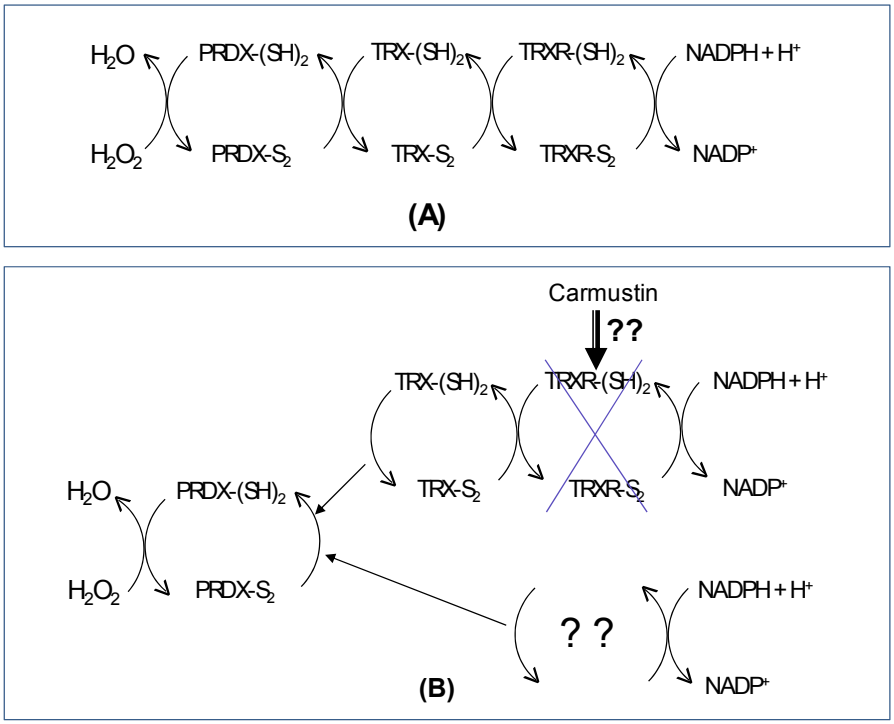
H2O
PRDX-(SH)2
TRX-(SH)2
TRXR-(SH)2
NADPH + H+
H2O2
PRDX-S2
TRX-S2
TRXR-S2
NADP+
(A)
Carmustin
??
TRX-(SH)2
TRXR-(SH)2
NADPH + H+
TRX-S2
TRXR-S2
NADP+
H2O
PRDX-(SH)2
H2O2
PRDX-S2
? ?
NADPH + H+
NADP+
(B)

Fig. 6.